

## PAPER

## High Gain Antipodal Fermi Antenna with Low Cross Polarization

Hiroyasu SATO<sup>†a)</sup>, Yukiko TAKAGI<sup>††\*b)</sup>, Members, and Kunio SAWAYA<sup>†</sup>, Fellow

**SUMMARY** Antipodal Fermi antenna (APFA) that uses an antipodal feeding section is proposed and its fundamental characteristics are presented. It is shown that the cross polarization level is decreased by 5–10 dB by the presence of the corrugation. It is also found that high gain, low VSWR and low side lobes and low back lobes are obtained. The mechanism of operation principles is discussed by using FDTD analysis. It is found that the corrugation transforms the current of parallel line mode to the current of traveling wave radiation mode and the effective aperture is enlarged which yields high gain characteristics.

**key words:** tapered slot antenna, TSA, Fermi antenna, broadband antenna, UWB antenna

## 1. Introduction

Recently, there is a great demand for broadband directive antennas for applications such as Ultra-wideband (UWB) communications, EMI measurements and wideband radars. Among the many types of broadband antennas such as the bow-tie antenna, the log-periodic dipole array antenna, the spiral antenna, the TEM horn antenna and the double rigged horn antenna, the tapered slot antenna (TSA) is well known as it offers thin structures, low weight, ease of fabrication, and is well suited for microwave integrated circuits (MICs). In order to maintain the broadband characteristics of TSA, it is important to design TSA geometry including the taper profile and the balun section for the feeding line to slot line transition.

Several taper profiles such as the LTSA (Linearly TSA), the CWSA (Constant Width Slot Antenna) and the BLTSA (Broken Linearly TSA) have been proposed [1]. Also several baluns for MSL-slot transition [1], CPW-slot transition [2], [3] have been discussed. Antipodal TSA [4], which uses both side of the substrate and directly merges the MSL into the taper section without using the stub was proposed. The antipodal TSA has broadband characteristics unlike the balun which use electromagnetic coupling [1]–[3], however, the higher cross polarization level is the problem which is caused by the antipodal geometry. In order to reduce the cross polarization level, Langley et al. introduced

balanced antipodal geometry which use 3 layered taper fed by strip-line to cancel the cross polarization components [5]. Kim et al. uses 2 antennas placed to be mirrored images each other [6].

Recently, Sugawara et al. proposed a TSA called “Fermi antenna” [7] having a profile defined by the Fermi-Dirac function as well as the corrugation on the side of the substrate. In our previous paper [8], [9], the design of the Fermi antenna for passive millimeter wave imaging have been performed and the relation between the parameters of the Fermi antenna and the radiation pattern has been investigated to obtain axially symmetric pattern suitable for lens optics.

In this paper, the antipodal Fermi antenna (APFA) with antipodal feeding section is proposed [10] and fundamental characteristics of APFA are presented. It is also shown that the cross polarization level decreases by the presence of the corrugation. The mechanism of operation principles is discussed by using FDTD analysis.

## 2. Geometry of APFA

Figure 1 shows the geometry of APFA. The E-plane is  $xz$ -plane and the H-plane is  $xy$ -plane, respectively. The Fermi-Dirac taper is determined by

$$f(x) = \frac{a}{1 + e^{-b(x-c)}} \quad (1)$$

where  $a$  denotes the asymptotic value of the width of the

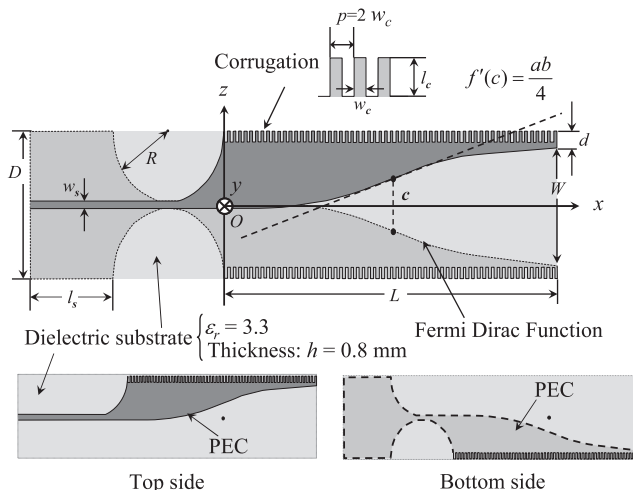


Fig. 1 Geometry of APFA with corrugation.

Manuscript received November 16, 2010.

Manuscript revised April 1, 2011.

<sup>†</sup>The authors are with the Graduate School of Engineering, Tohoku University, Sendai-shi, 980-8579 Japan.

<sup>††</sup>The author was with the Graduate School of Engineering, Tohoku University.

\*Presently, with NTT DoCoMo R&D Center, Yokosuka-shi, 239-8536 Japan.

a) E-mail: sahiro@ecei.tohoku.ac.jp

b) E-mail: takagiy@nttdocomo.co.jp

DOI: 10.1587/transcom.E94.B.2292

**Table 1** Parameters of APFA.

Dimensions	[mm]	$[\lambda_0]$ @10GHz	Number of Cells
Length of antenna $L$	120	4	$300\Delta x$
Width of aperture $W$	30	1	$120\Delta z$
Width of substrate $D$	42	1.4	$168\Delta z$
Thickness of substrate $h$	0.8	0.027	$4\Delta y$
Length of corrugation $l_c$	5	0.167	$20\Delta z$
Width of corrugation $w_c$	0.8	0.027	$2\Delta x$
Pitch of corrugation $p$	1.6	0.056	$4\Delta x$
Width of MSL $w_s$	2	0.067	$8\Delta z$
Length of MSL $l_s$	30	1	$75\Delta x$
Distance between edges of aperture and substrate $d$	6	0.201	$24\Delta z$
Radius of balun $R$	20	0.667	$50\Delta x$

$\Delta x = 0.4$  mm,  $\Delta y = 0.2$  mm,  $\Delta z = 0.25$  mm  
 $a = 15$  mm,  $b = 2.4/\lambda_0$ ,  $c = 60$  mm,  $2a = W$ ,  $f(c) = a/2$

taper for  $x \rightarrow \infty$  and  $c$  denotes the position of the inflection point of the Fermi-Dirac function. Because of the relation of  $f'(c) = ab/4$ ,  $b$  is related to the gradient at the inflection point  $c$ . Also there is a relation of  $f(c) = a/2$  and  $W = 2a$  when  $b(L - c) \gg 1$  where  $L$  is the length of antenna.

Table 1 shows the parameters of APFA used in the design, where  $h$  is the thickness of the substrate. FDTD analysis and the measurement were performed in the frequency range of 2 GHz to 18 GHz. In the analysis, the cell size are  $\Delta x = 0.4$  mm,  $\Delta y = 0.2$  mm and  $\Delta z = 0.25$  mm and the analysis space is  $244.4$  mm  $\times$   $20.8$  mm  $\times$   $80$  mm. The number of time steps was 30,000 and the 8-layer PML was used. The antenna is separated  $40\Delta x$ ,  $20\Delta y$  and  $60\Delta z$  from the PML in each direction. A Gaussian pulse was used for the excitation of the MSL and the four cell feed between the strip conductor and the ground plane was used with  $50\Omega$  internal resistance. The current at the feed point was calculated by using.

Ampere’s law and magnetic frill around cells. In order to determine the parameters of APFA, a procedure similar to the design of 35 GHz band coplanar Fermi antenna designed in [8], [9] was employed and a lot of calculations were performed.

The measurement of the actual gain was performed comparing its gain with those of 4 standard gain horn antennas with different frequency band (3.94–5.99 GHz, 5.38–8.18 GHz, 8.20–12.5 GHz and 11.9–18.0 GHz). Input impedance, radiation pattern and gain were measured in an anechoic chamber using the vector network analyzer Agilent 8722 ET.

**3. Numerical and Experimental Results**

VSWR of APFA without and with the corrugation are shown in Fig. 2 and Fig. 3, respectively. It is observed that the calculated VSWR almost agree with the measured data. In the case with the corrugation, the measured VSWR is less than 2 in a frequency range of 5.76 GHz to 14.3 GHz and relative bandwidth of about 1:2.5 is obtained. On the other hand, VSWR without the corrugation is larger than 2 in a broad

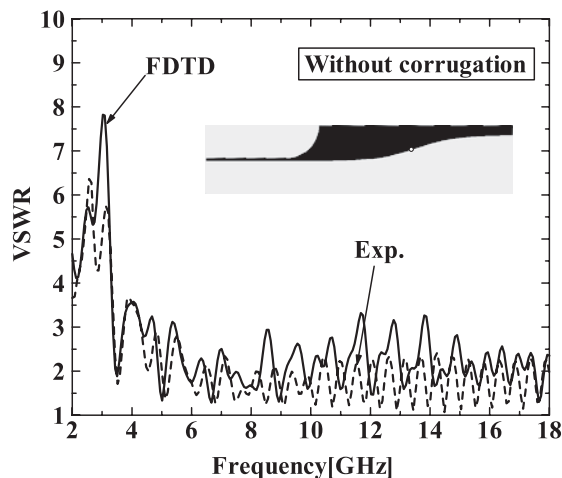


**Fig. 2** VSWR of APFA without corrugation.

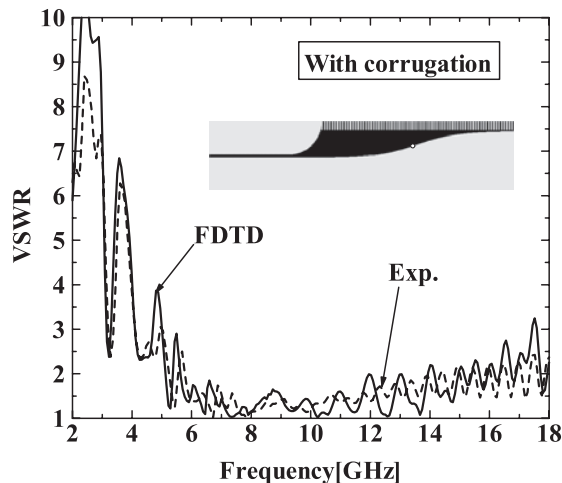


**Fig. 3** VSWR of APFA with corrugation.

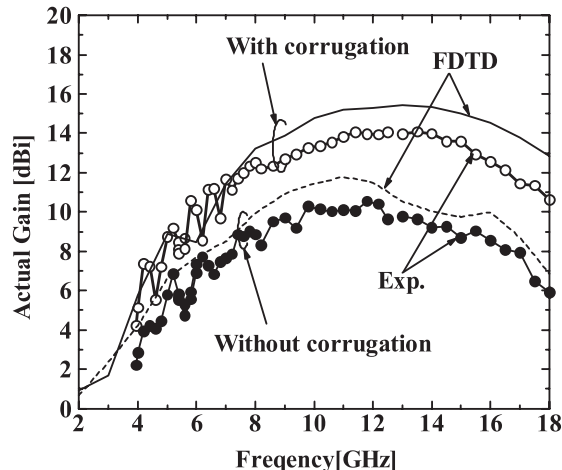


**Fig. 4** Actual gain of APFA with and without corrugation.

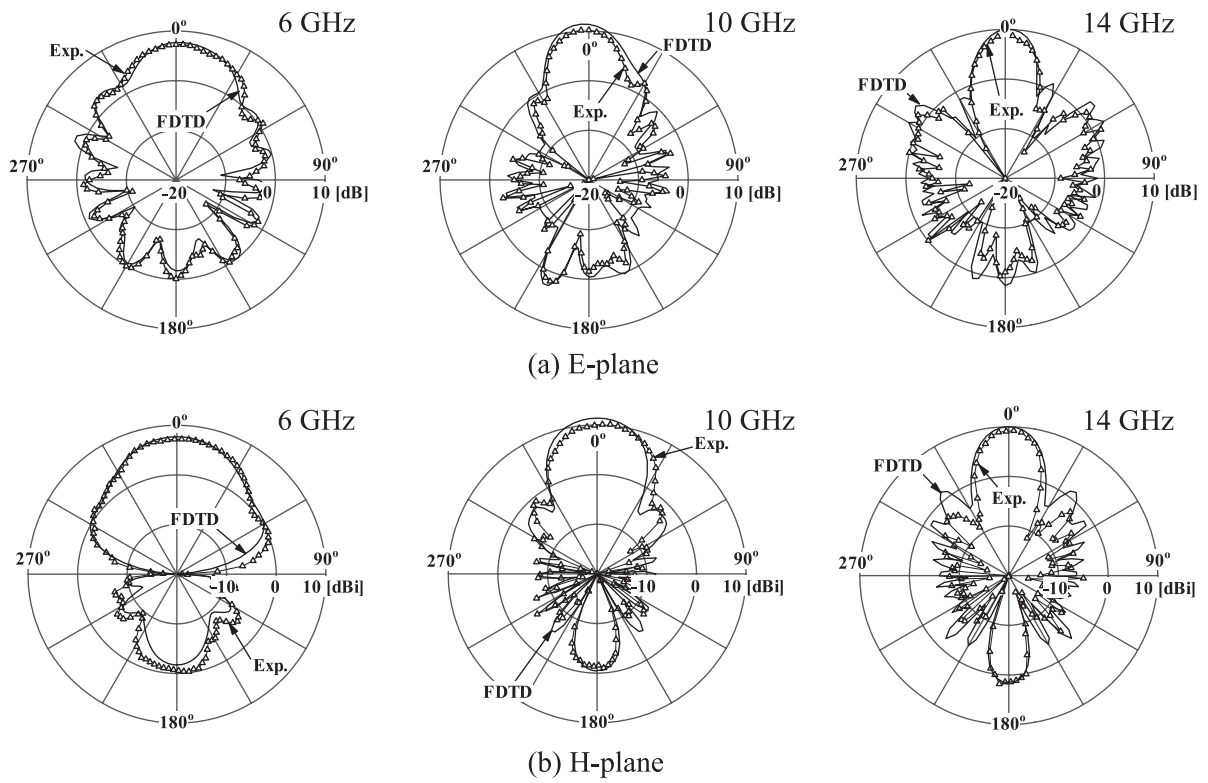


Fig. 5 Actual gain pattern of APFA without corrugation.

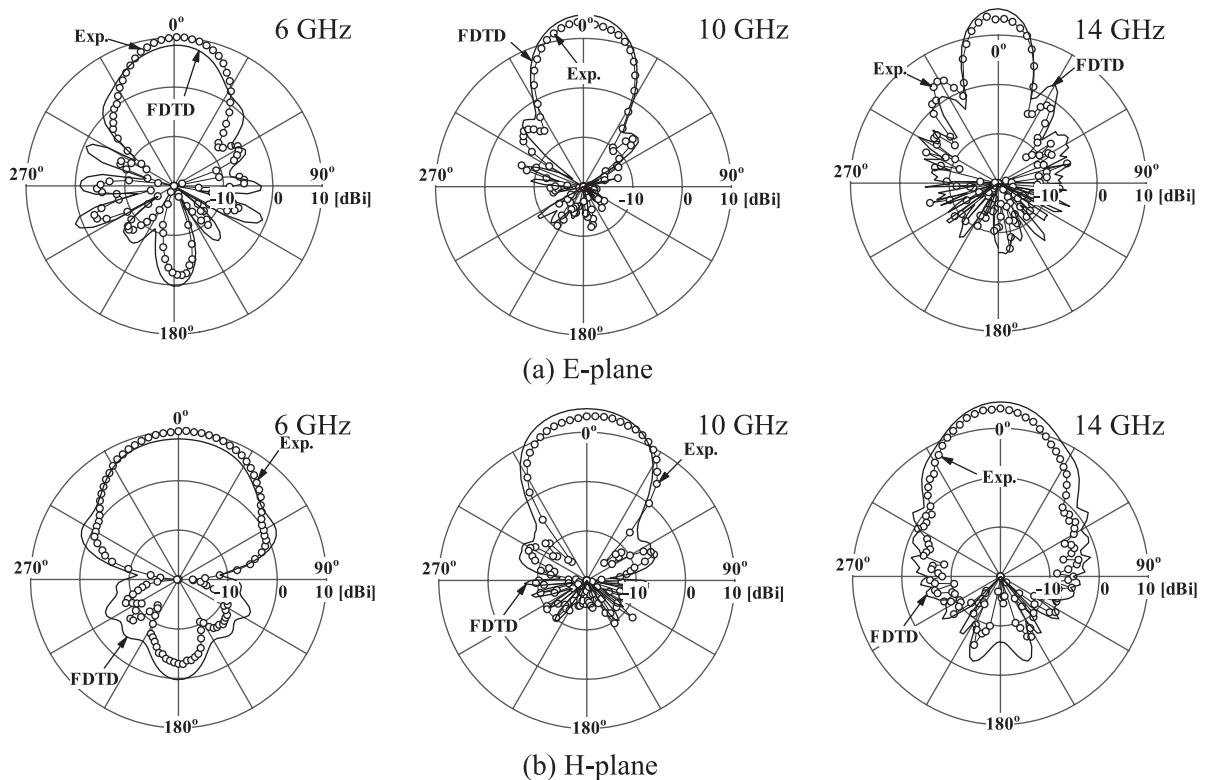
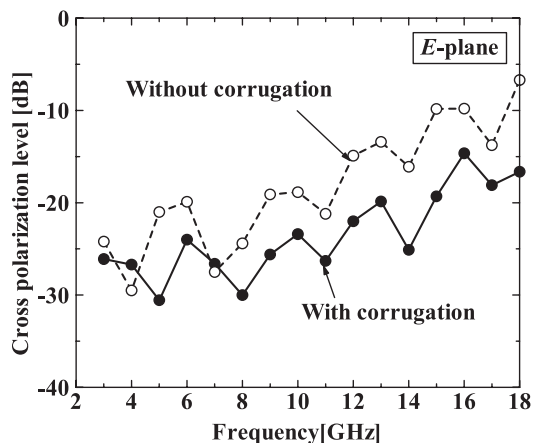
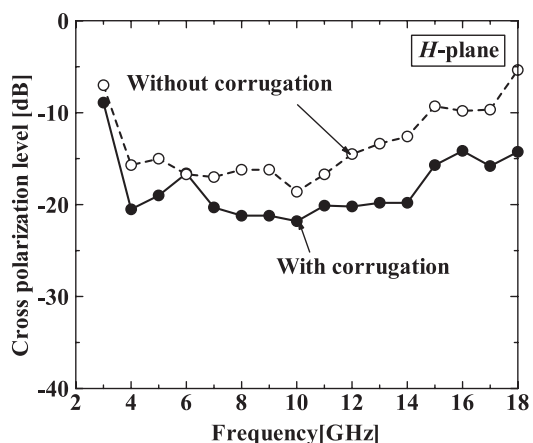


Fig. 6 Actual gain pattern of APFA with corrugation.

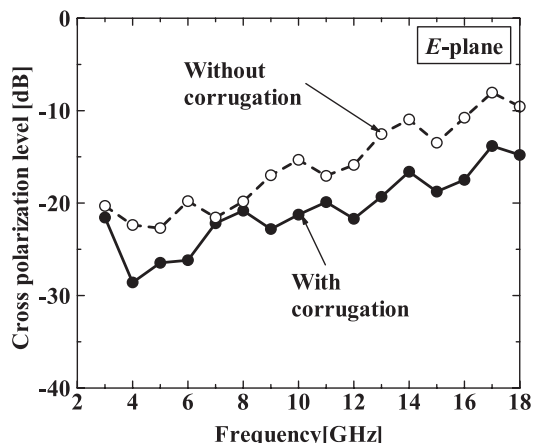


(a) E-plane

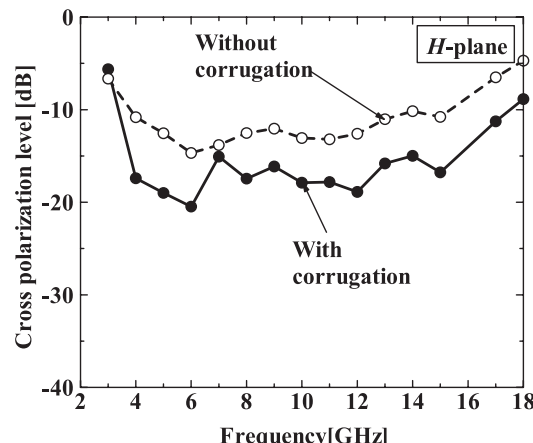


(b) H-plane

Fig. 7 Calculated cross polarization level of APFA.



(a) E-plane



(b) H-plane

Fig. 8 Measured cross polarization level of APFA.

frequency range.

The actual gain of APFA with and without the corrugation are shown in Fig. 4. The calculated values are 1–2 dB higher than the measured values and the difference between them becomes large in a frequency region of 8–18 GHz. These results might be caused by the copper loss and dielectric loss which are not considered in FDTD analysis. The gain in the case with the corrugation is higher than the case without the corrugation in the broadband frequency range. The values of calculated actual gain in the cases with and without the corrugation at 10 GHz are 14.8 dBi and 11.4 dBi, respectively. The maximum gain of 15.5 dBi is observed at 13 GHz and the gain decreases in higher frequency region.

Figure 5 and Fig. 6 show the actual gain patterns of APFA without and with the corrugation, respectively. It is observed that the numerical results agree with the experimental data. Axially asymmetric side lobes in the E-plane are observed for both cases which are caused by the asymmetric geometry of antipodal taper section. The large back lobe levels are observed in the case without the corrugation, however, they decrease by the presence of the corrugation for both the E-plane and the H-plane. The side lobe levels of -19.3 dB and -19.5 dB in the E-plane and the H-plane

are obtained in the case with the corrugation at 10 GHz.

The calculated and measured cross polarization level of APFA with and without the corrugation is shown in Fig. 7 and Fig. 8, respectively. In the case without the corrugation, the cross polarization levels in the E-plane and the H-plane are less than -10 dB in the frequency range of 3.6 GHz to 15 GHz. In the case with the corrugation, the cross polarization levels are less than -15 dB for 3 GHz to 16 GHz and the improvement of 5 dB and the effect of the corrugation are observed.

#### 4. Mechanism of High Gain Characteristics

In order to investigate the mechanism of improved VSWR and enhanced radiation characteristics by the presence of the corrugation, the distributions of the current and the electric field were calculated. Figure 9(a) shows the distribution of  $x$  and  $z$  components of the current on the top side of conducting  $xz$  plane in the cases without the corrugation. A strong standing wave of  $J_x$  is observed not only on the micro-strip line and the Fermi taper edges but also on the side of the conducting plane between the inflection point ( $x = c = 60$  mm) and the aperture line of antenna ( $x = L$ ) are observed, and

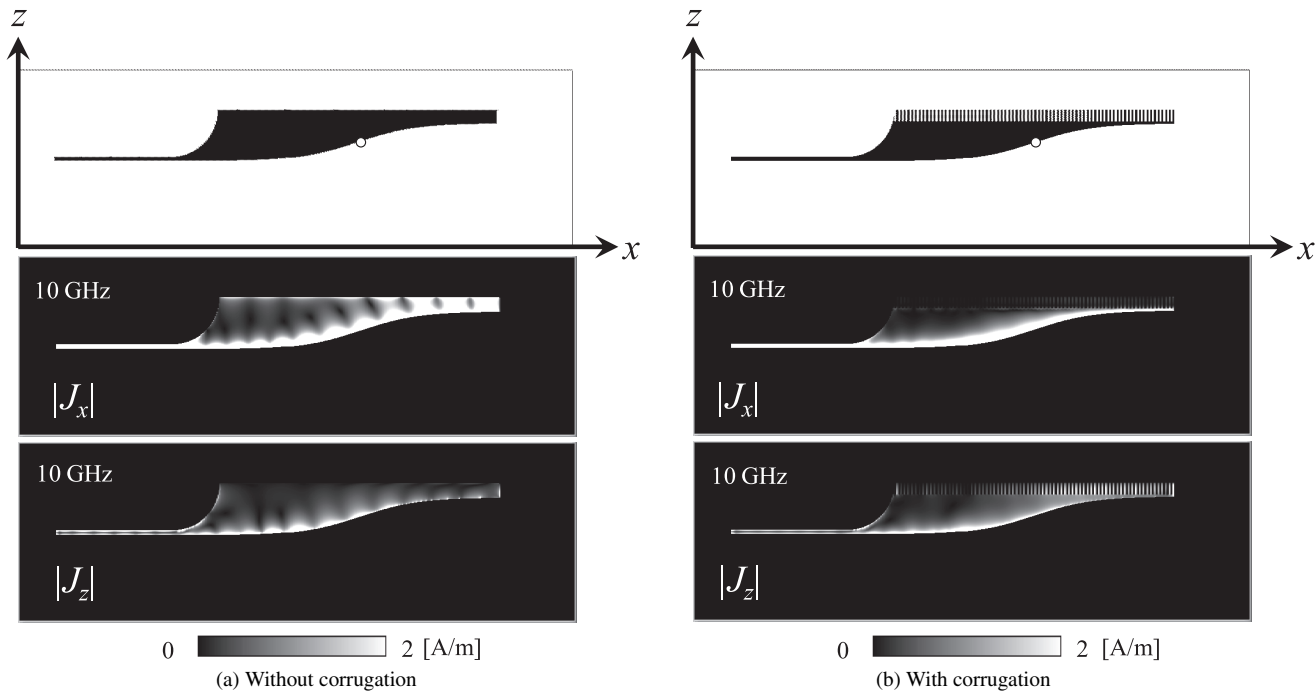


**Fig. 9** Distributions of  $x$  and  $z$  components of current on the top side of conducting  $xz$  plane in cases with and without corrugation.

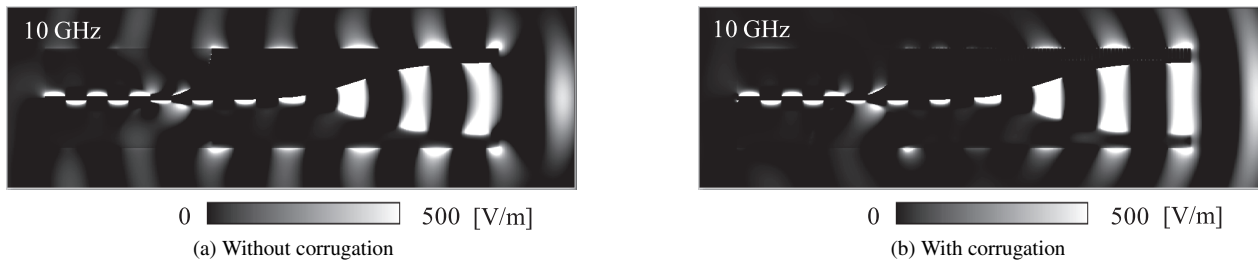


**Fig. 10** Distributions of real part of electric field  $E_z$  on  $xz$  plane in cases with and without corrugation.

$J_z$  attenuates along the direction of the aperture. By these observations, APFA without the corrugation is considered to be similar to an open-ended parallel line and VSWR becomes high. Figure 9(b) shows the distributions of  $x$  and  $z$  components of the current on the top side of conducting  $xz$  plane in the cases with the corrugation.  $J_x$  on the taper edge is suppressed and strong  $J_z$  appears along the corrugation. It is considered that these results explain that the corrugation transforms the current of parallel line mode ( $J_x$ ) into the current of traveling wave radiation mode ( $J_z$ ). Thus, the improvement of VSWR and lower side lobes are obtained.

Figure 10(a) and Fig. 10(b) show the distribution of real part of the electric field  $E_z$  on  $xz$  plane in the cases without and with the corrugation, respectively. The phase difference between the electric field inside and outside of the taper slot is almost  $180^\circ$  and the width of the effective aperture is small. On the other hand, the phase inside the taper slot is almost the same to that outside of the taper slot and the effective aperture is enlarged by the presence of the corrugation. It is considered that these results explain that the

corrugations enhance the gain of antenna.

## 5. Conclusion

APFA with the combination of antipodal feeding section and Fermi taper section was proposed. The calculated actual gain of 14.8 dBi was obtained at 10 GHz with low cross polarization levels of  $-23.4$  dB in the E-plane and  $-21.8$  dB in the H-plane. Measurements show that the cross polarization decreases by 5–10 dB in the E-plane and the H-plane by the presence of the corrugation. It was also found that VSWR, side lobes and back lobes decrease. The mechanism of operation principles is investigated by the distribution of the current and electric field obtained by using FDTD analysis. It was found that the corrugation transforms the current of parallel line mode into the current of traveling wave radiation mode and the effective aperture is enlarged which yields high gain characteristics.

## References

- [1] H.F. Lee and W. Chen, *Advances in microstrip and printed antennas*, Chapter 9, John Wiley & Sons, 1997.
- [2] T.Q. Ho and S.M. Hart, "A broad-band coplanar waveguide to slotline transition," *IEEE Microwave and Guided Wave Letters*, vol.2, no.10, pp.415–416, 1992.
- [3] K.P. Ma, Y. Qian, and T. Itoh, "Analysis and applications of a new CPW-slotline transition," *IEEE Trans. Microw. Theory Tech.*, vol.47, no.4, pp.426–432, 1999.
- [4] E. Gazit, "Improved design of the Vivaldi antenna," *IEE Proc. H*, vol.135, no.2, pp.89–92, 1988.
- [5] J. Langley, P. Hall, and P. Newham, "Balanced antipodal Vivaldi antenna for wide bandwidth phased arrays," *IEE Proc. Microwaves, Antennas and Propagation*, vol.143, pp.97–102, 1996.
- [6] S.G. Kim and K. Chang, "A low cross-polarized antipodal Vivaldi antenna array for wide-band operation," *IEEE AP-S Int. Symp. Dig.*, vol.3, pp.2269–2272, Monterey, 2004.
- [7] S. Sugawara, Y. Maita, K. Adachi, K. Mori, and K. Mizuno, "A mm-wave tapered slot antenna with improved radiation pattern," *IEEE MTT-S Int. Microw. Symp. Dig.*, pp.959–962, Denver, 1997.
- [8] H. Sato, N. Arai, Y. Wagatsuma, K. Sawaya, and K. Mizuno, "Design of Millimeter Wave Fermi Antenna with Corrugation," *IEICE Trans. Commun. (Japanese Edition)*, vol.J86-B, no.9, pp.1851–1859, Sept. 2003.
- [9] H. Sato, K. Sawaya, Y. Wagatsuma, and K. Mizuno, "Broadband FDTD analysis of Fermi Antenna with Corrugation," *IEICE Trans. Commun. (Japanese Edition)*, vol.J88-B, no.9, pp.1682–1692, Sept. 2005.
- [10] Y. Takagi, H. Sato, Y. Wagatsuma, K. Sawaya, and K. Mizuno, "Study of high gain and broadband antipodal Fermi antenna with corrugation," *Proc. 2004 Int. Symp. Antennas and Propagation, ISAP'04*, vol.1, pp.69–72, Sendai, 2004.



**Kunio Sawaya** received the B.E., M.E., and D.E. degrees from Tohoku University, Sendai, Japan, in 1971, 1973 and 1976, respectively. He is presently a Professor in the Department of Electrical and Communication Engineering, Tohoku University. His areas of interests are antennas in plasma, antennas for mobile communications, theory of scattering and diffraction, antennas for plasma heating, and array antennas. Dr. Sawaya is a member of the Institute of Image Information and Television Engineers of Japan. He received the Young Scientists Award in 1981, the Paper Award in 1988, the Communications Society Excellent Paper Award in 2006, and the Zen-ichi Kiyasu Award in 2009, all from the IEICE. He served as the Chairperson of the Technical Group of Antennas and Propagation of IEICE from 2001 to 2003, the Chairperson of the Organizing and Steering Committees of 2004 International Symposium on Antennas and Propagation (ISAP'04), and the President of the Communications Society of IEICE from 2009 to 2010.



**Hiroyasu Sato** received the B.E. and M.E. degrees from Chuo University, Tokyo, Japan, in 1993 and 1995, respectively and the D.E. degree from Tohoku University, Sendai, Japan, in 1998. He is presently an Assistant Professor with the Department of Electrical Communications, Tohoku University. His area of interests computational electromagnetics, antennas in plasma, antennas for plasma production, broadband antennas and millimeter wave imaging.



**Yukiko Takagi** received the B.E. and M.E. degrees from Tohoku University, Sendai, Japan, in 2003 and 2005. In 2005, she joined NTT DoCoMo, Inc., where she has been engaged in research and development of mobile communication systems for LTE.